AIRCRAFT COMPLETE CONFIGURATION EXPERIMENTAL ANALYSIS OF THE ITA's UNMANNED AERIAL VEHICLE

Roberto da Mota Girardi
Instituto Tecnológico de Aeronáutica (ITA). Praça Mal. Eduardo Gomes, 50, S J Campos – SP, Brasil
girardi@ita.br

André Valdetaro Gomes Cavalieri
Instituto Tecnológico de Aeronáutica (ITA). Praça Mal. Eduardo Gomes, 50, S J Campos – SP, Brasil
andre@ita.br

Tiago Barbosa de Araújo
Instituto Tecnológico de Aeronáutica (ITA). Praça Mal. Eduardo Gomes, 50, S J Campos – SP, Brasil
araujotb@ita.br

Abstract. *The unmanned aircraft vehicle (UAV) considered in this work has the specific mission of examining elements of an electric energy transmission line (the tower, vegetation at the neighbor area and the electric cables). Such aircraft has some particular characteristics: (i) a relatively small velocity, that is, low Reynolds number, (ii) different material and manufacturing techniques are used and (iii) the weight is very low and, therefore, the aircraft will be very sensitive to atmospheric gusts. Such characteristic increases the difficulty to accomplish the mission, that is, performing a pre-defined path along a transmission line and its elements imaging. In order to improve the aircraft performance analysis, the lift coefficient as a function of the angle of attack and the drag polar of the trimmed aircraft must be determined. In the present paper a large amount of experimental data is presented and used to obtain aerodynamic curves mentioned above. One of the most important parameters to allow aircraft stability is the aerodynamic center position (Xca)and such parameter is calculated by using the experimental results mentioned above. Experiments and a semi-empirical method, normally used in the conceptual design phase, are compared and some indications to improve this method are verified and they can be used to implement improvements to the method mentoned above. The experiments were performed at the ITA's Wind tunnel and half models were used.*

Keywords*: Unmanned Aircraft Vehicle, aircraft complete configuration, Trimmed aircraft aerodynamic curves, Aerodynamic center determination*

1. INTRODUCTION

Unmanned aircraft vehicles (UAV) can be used in several civil applications, like that: (i) Electrical lines and pipelines examination, (ii) harbors, forest reservations and less accessible frontiers vigilance, (iii) aircraft and disappeared people rescue, (iv) aerial picture generation and (v) others.

In 2004 Technological Institute of Aeronautics (ITA) was contacted to participate in a cooperation involving Advanced System Studies Center of Recife (CESAR) and São Francisco Electric Company (CHESF). The goal of such cooperation was an UAV development, for electrical line elements (towers, vegetation existing in the neighborhood of electrical lines, electrical connectors at the towers and etc) examination. In order to accomplish this task, a very low velocity (80 km/h) aircraft, flying at low altitude, is required, due to infrared camera limitations (required to observe hot spots, which indicate electric problems at some line elements). In such velocity range, atmospheric gusts became very important due to these effects on the flight security and because the electric line elements examination mission became very difficult, due the constant aircraft attitude changes.

The low aircraft velocity, required to accomplish the infrared camera examination mission, is in the inferior limit of an airplane flight envelope, because a high wing loading (W/S) is necessary to give the aircraft a low sensibility to atmospheric gusts, but, on the other hand, a low value of W/S is required to accomplish the low velocity flight requirement. All mission requirements could be fulfilled by using other kinds of aircrafts, like a helicopter, a dirigible or a hybrid vehicle, that is, a mixture between a dirigible and an airplane, for example. The most adapted kind of aircraft was analyzed by Girardi and Rizzi (2005a), where an airplane was chosen to be the kind of aircraft used in this project.

The second step in the conceptual phase of the airplane project was the definition of the more adapted configuration, considering all requirements fulfillment. Two basic airplane configurations were considered: (i) in the first one the engine is located at the airplane nose, a conventional tail was chosen to give stability and control to the aircraft and the camera was located at the fuselage low surface, near the aircraft gravity center (GC). (ii) In the second configuration, the engine was located at the fuselage tail, in the pusher configuration, and two booms were used to assembly the tail to the wing. In this configuration, the camera could be located at the fuselage nose or in the same place of the first configuration. Both configurations have high wing position (relative to the fuselage), a tricycle landing gear type and a rectangular wing. These configurations were analyzed by Girardi and Rizzi, (2005b) and the first one was

chosen, considering the camera position near the aircraft GC (better to decrease effects on the camera due to the aircraft constant attitude changes, associated to the gusts effects) and the design team experience.

The aircraft conceptual design phase was executed by the Aeronautics Department of ITA and a special methodology was developed (Girardi e Rizzi, 2006) to face the problems associated to the airplane specific mission, that is, image acquisition from an aircraft at low velocity, manufactured with non conventional material and subjected to atmospheric gusts, because of the low altitude required by the infrared imaging. In such methodology, the aircraft dimensions were determined considering the autopilot characteristics and this is an important aspect of the procedure adopted to this UAV design.

The work reported in this paper is inserted into the preliminary design phase, where more accurate information has to be used in order to improve the analysis methods used to determine the airplane dimensions, as well as, the relative positions of the different aircraft parts (wing, fuselage and tail). One of the problems verified during the conceptual design phase was the lack of information on low Reynolds number aerodynamic data, required to a small vehicle at low velocity. Such kind of information is very useful to generate the aircraft characteristic curves (CL x α, CL x Cm and the drag polar), which are used to performance, as well as, stability and control calculations.

During the aircraft design conceptual phase, the aerodynamic characteristics of the complete configuration, that is, wing, fuselage and tail, are generated by using a semi-empirical methodology (Roskam, 1993, and Raymer, 1999), where fuselage is considered a body of revolution and the airplane parts interference are calculated by using empirical factors, which do not consider the actual way the aircraft parts are joined together. It is important to note that such factors were obtained to full scale airplanes, where Reynolds number is high.

The actual UAV fuselage is not a body of revolution. It has a rectangular cross section and, along its length, it is constituted by: (i) a small nose, containing the engine and its support, (ii) a constant cross section area part, where fuel tank, parachute, cameras, electronic equipment for guidance and control and batteries are installed and, finally, (iii) a trailing cone, characterized by a cross section area reduction, performed with the lower surface inclination. The upper trailing cone surface is in the same plane of the constant cross section area part of the fuselage. In such kind of fuselage, longitudinal vortices can be generated due to the abrupt area variation at the trailing cone interface, resulting induced drag and lift variations. The wing is positioned at the fuselage upper surface and flow interference can be observed at the corner formed by the union of these aircraft parts. Other source of uncertainty is the downwash velocity at the horizontal tail, induced by the wing flow, which is estimated by using semi-empirical formula during the conceptual design phase. This parameter is very important to determine the aircraft aerodynamic center, as well as, the horizontal tail incidence angle.

The objective of this paper is to present experimental results to the aerodynamic characteristic curves of the UAV complete configuration, at low Reynolds number. The experiments were performed in an open circuit wind tunnel and a three component balance was used to obtain lift, drag and pitch moment of a half model (balance is assembled at the wind tunnel lateral wall). Wool tufts were used to allow flow visualization of the model at several angles of attack, in order to generate information to perform experimental result analysis. The questions discussed above are considered during the experimental results analysis and the aerodynamic center is obtained directly from the results.

Finally, the experimental results are compared with the semi-empirical methodology mentioned above to verify its applicability to the specific fuselage used for the UAV developed at ITA. This comparison allows modification of the semi-empirical method and, therefore, more reliable aerodynamic characteristic curves could be generated to future fuselage, with similar shape and subjected to a flow with similar Reynolds number.

2 EXPERIMENTAL APPARATUS

The measurements were performed in a blower wind tunnel with square test section, characterized by a dimension of 460 mm. The flow velocity ranges from 4 to 30 m/s and the turbulence intensity is 0.5% at the maximum velocity. Along the test section length the cross section area is changed in order to compensate the boundary-layer growth and, as a consequence, to keep a constant static pressure. This area change is performed by filling the test section corners with triangular elements, whose dimension changes along test section length, as shown in the Fig. 1.

Lift, drag and pitch moment of a model are measured with a balance fixed at the test section lateral wall (outside the wind tunnel). Aerodynamic forces and moment on the model are transmitted to the balance through a metal axis. Such balance has a triangular plate used to fix the metal axis originated at the model. The triangular plate is connected to the wind tunnel structure by using three load cells (metal plates, instrumented with four strain gages each, in order to assembly a complete Wheatstone bridge). Two of these load cells are used to make measurement of lift and pitch moment (sensors A and F) and the third one is used to obtain drag force measurements (sensor D). Each load cell is connected to an independent signal conditioner module (amplifier and filter), which allows adjustment of the output voltage considering the data acquisition board characteristics. For the present experiment, the maximum output voltage of each sensor is chosen to be 10 volts, which maximize measurements resolution.

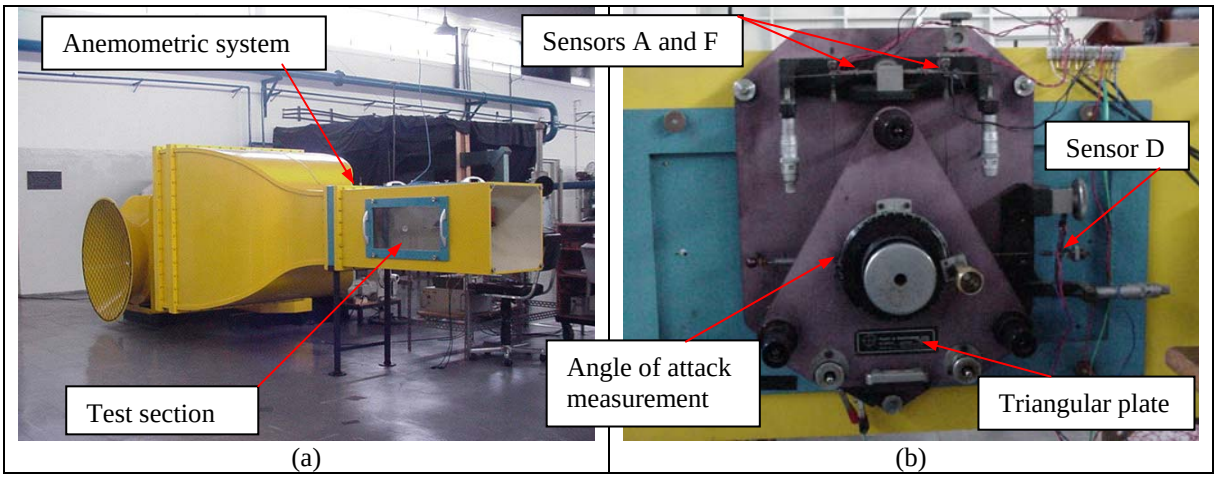

Figure 1: (a) Open circuit wind tunnel and (b) three component aerodynamic balance.

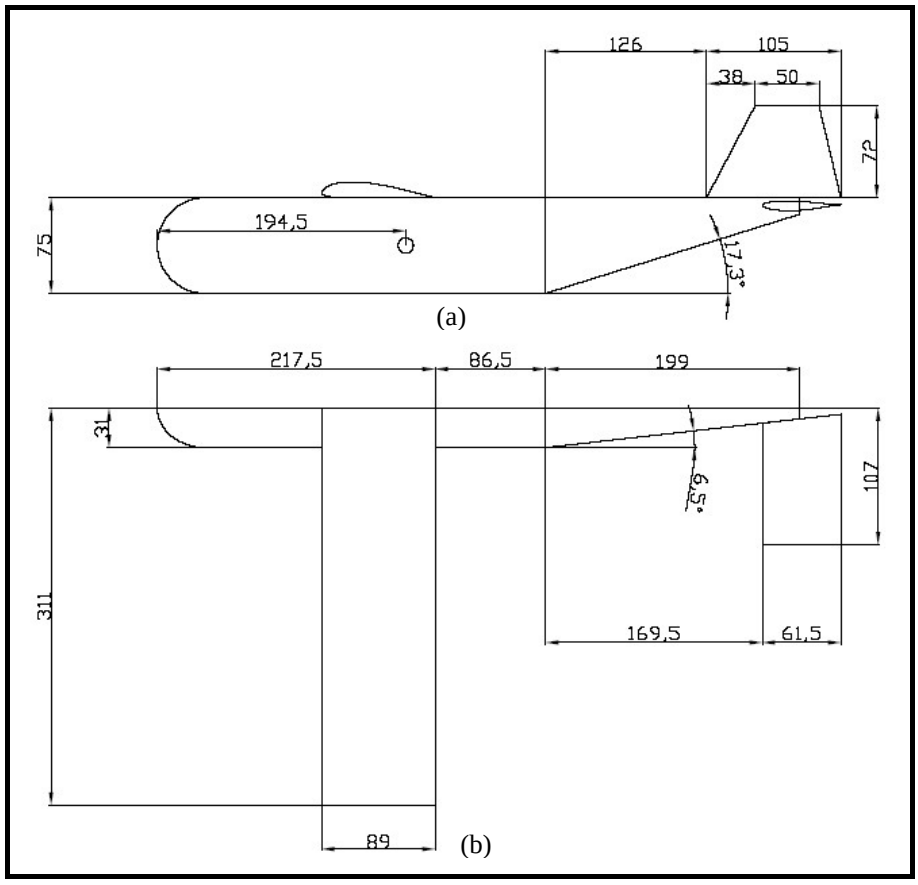

Figure 2: Half model of the complete configuration: (a) Lateral view and (b) plan view . Dimensions in mm.

The dynamic and static pressures are measured by using a Pitot tube located at the beginning of the test section (tunnel anemometric system), just after the end of the contraction section, as can be seen in the figure 1(a). Pressure transducers are connected to the Pitot tube and a signal conditioner is used to amplify the output voltages before the connection with the data acquisition board.

The model angle of attack is varied manually and its measurement is performed by a rotating device (where the model axis is fixed) divided in 360 equal parts. The uncertainty of ± 0.5 degrees can be considered to this measurement.

Due to the balance configuration, the aerodynamic tests have to be performed with a fuselage half model, as shown in the figure 2. The complete configuration model was manufactured with wood and it has the following characteristics: (i) a fuselage a small nose region, a constant rectangular cross section part, with 75 mm high and 31 mm width and a trailing cone, where the cross section area decreases along the model longitudinal axis, (ii) a rectangular wing with aspect ratio equal to 7. A Selig SD7062 airfoil is used and the wing is positioned at the fuselage upper surface, with 2.4 degrees incidence angle. (iii) A Selig S8052 airfoil is used at the rectangular horizontal tail, with

aspect ratio equal to 3.5. A variable horizontal tail is allowed in order to analyze the aircraft trim and the downwash velocity induced by the wing fuselage configuration. (iv) A NACA 0012 is used at the vertical tail. This lifting surface is characterized by the following non-dimensional parameters: 1.0 aspect ratio, 0.48 taper ratio and 26 degrees sweep back angle for the leading edge. (v) Landing gears were not considered in the present tests. The model is 503 mm total length and a steel axis is fixed at 194,5 mm from the model nose and it is used to fix the model to the aerodynamic balance. The fuselage frontal area is 0.0023 m^2. Considering the test section cross section area, the model blockage ratio is approximately 1,1% and, therefore, the test section walls interference on the model flow is very low.

For half model testes, the model symmetrical plane (wind tunnel wall) should be a flow stream plane and the wall boundary layer flow should be eliminated to accomplish rigorously such requirement. One end plate is used to isolate the wind tunnel boundary layer from the flow over the fuselage model, in order to approximate the flow over the model to the free flight flow. The experimental results reported by Kubo [8], were used, initially, to define the end plates dimensions. The distance the end plate is fixed from the wind tunnel lateral wall is defined as a function of the boundary layer thickness, determined in a previous work [11] by using a hot wire anemometer.

After experiments conducted with an airfoil model, a flow field between the two sides of the end plates was observed, generating longitudinal vortices along the upper and lower edges of the end plate and causing great disturbances on the model flow. Such problem is discussed in Girardi et alli (2007) and the problem was solved with an end plate spanning the test section high, to avoid flow communication through the upper and lower edges of the end plate. The same end plate configuration was used in the present work.

3. EXPERIMENTAL PROCEDURE

In the present work, the following measurements have to be performed: (i) the forces and pitch moment of the complete model configuration, (ii) the dynamic pressure, necessary to obtain the non-dimensional coefficients for lift (C_L), drag (C_D) and pitch moment (C_M). In this paper section, the experimental procedure established to determine each one of the above parameters is described, in order to show all care taken to guarantee reliable results.

As mentioned in the preceding section, lift, drag and pitch moment are measured by using an aerodynamic balance, with three load cells. The first task to be done is the load cells calibration, in order to obtain a correlation between the force acting on each load cell with the voltage read by the acquisition system. The calibration procedure is performed by incrementing loads from zero to the maximum value estimated for the specific sensor of the balance and, after that, a decrement is done up to zero again. At least 20 measures are used for the calibration process, in order to determine statistic parameters, used to uncertainties estimates. During such procedure, a small amount of vibration is used to decrease the time required to the balance structural parts accommodation and it is worth to note that such vibration is kept during the sampling process, performed by the data acquisition system. In the calibration procedure, one thousand measures were performed during a sampling time of one second and just a value (average of 1000) of voltage is correlated to the force imposed on the load cell. Each balance sensor is loaded by using calibrated masses and a system constituted by cables and pulleys, responsible to apply the force to an axis connected to the balance. The three balance sensors are calibrated in two steps: (i) the load cell associated to the drag force is calibrated alone but (ii) for the other two sensors, the vertical load applied to the axis connected to the balance is divided by two and the load cells associated to the lift and pitch moment are calibrated simultaneously.

At the region where anemometric system is located (at the beginning of the test section) the flow field is distorted, due to the area variation along the contraction, causing errors in the values measured for the dynamic and static pressures. This problem can be corrected by performing a calibration procedure, where a Pitot tube, placed at the test section central region (location where models are tested) is compared with the anemometric system fixed at the wind tunnel. Calibration curves for the dynamic and static pressures are the results of the above procedure and they are used to correct the experimental results obtained with the wind tunnel anemometric system (The Pitot tube at the test section central region is withdrawn during the model experiments). The above calibration curves are incorporated in a computer code used to make calculations of the aerodynamic coefficients.

As mentioned in the previous section, the dynamic pressure is measured by using a pressure transducer, ranging from zero to 100 mm of water. A Betz manometer, with least count of 0,1 mm of water, is used as standard for the pressure transducer calibration, which is performed in the following way: (i) Initially, the pressure is increased and decreased several times (minimum of three) in order to get a repeatable measure of zero gage pressure at the Betz manometer. With such procedure, the internal walls of the Betz manometer are wetted. (ii) Starting from zero, the pressure is increased up to 50 mm of water, in steps of 5 mm and then (iii) pressure is decreased, using the same steps, up to zero again. For each point of the calibration curve, one thousand measures are collected during one second after the pressure stabilization (observed at the Betz manometer). The data acquisition code, written in LabView ambient, presents the linear fit of the experimental data and the standard deviations associated with the uncontrolled parameters of the experimental setup (random errors). These parameters are used to estimate the uncertainties associated to the aerodynamic coefficients.

After the calibration phase was finished, the experiment can be run in the following manner: (i) the end plate is assembled inside the wind tunnel test section, whose longitudinal axis is stamped on the end plate surface in order to

allow model alignment. (ii) The model is fixed to the wind tunnel aerodynamic balance (through its metal axis) and initial alignment is performed, comparing the fuselage model upper surface with the longitudinal axis stamped on the end plate surface. (iii) Before starting the wind tunnel, all sensor signals are read by the data acquisition system (initial voltages). This operation is performed after some vibration was introduced, in a similar manner used during the aerodynamic balance calibration (see preceding section), in order to guarantee all load cells are well accommodated to the loads associated the zero dynamic pressure. The initial voltage accuracies are very important because all force measurements accuracies depend on them. It is worth to note that the aerodynamic forces and moments are obtained through the difference between the sensor signal (voltage), measured with wind tunnel turned on, and the initial voltage (obtained with flow velocity equal to zero). (iv) In the next step, wind tunnel is turned on and the dynamic pressure required to the specific test is established. (v) The following results are typically obtained in an aerodynamic test program: The drag polar (C_D x C_L), C_L x α and C_M x α. With the dynamic pressure fixed at a required value (associated to the Reynolds number) the angle of attack (α) is varied. In general, such variation starts at a negative angle of attack and increments of 1 degree are used. (vi) During the experiments described above, a data acquisition code, written in the LabView ambient, is used to make the measurements of the aerodynamic balance sensors (three) and the pressure transducer, used to register the wind tunnel dynamic pressure. For each angle of attack, whose value is inserted through the keyboard, the four sensor signals, are sampled 2000 times, using sampling rate of 200 hz. The resulting sample time of 10 seconds was chosen to account for the wind tunnel dynamic pressure variations and an average value is obtained for each parameter measured in this experiment. (vii) Data reduction is performed with other computational code, written in the LabView ambient, where the data generated to each sensor (voltages) is combined with the calibration curves to determine forces and moments acting on the model. Ambient pressure and temperature are used to calculate air density and dynamic viscosity. These parameters are combined with the dynamic pressure to calculate the test Reynolds number. Finally, the model reference area (wing area) together with the forces and moments are used to determine the aerodynamic coefficients mentioned previously.

Data generated during calibration procedure, as well as, during the experiment are used to determine the uncertainty associated to each aerodynamic coefficient. The uncertainty analysis was made by using the procedure described by kline and Mcintoch [7].

4. ANALYSIS OF RESULTS

In this work, a set of horizontal tail incidence angles (i_h) are used to obtain the characteristic aerodynamic curves of the complete configuration of the UAV analyzed at ITA. The main idea is to generate experimental information to perform the aircraft trim and, therefore, to calculate the C_L x α and the C_L x C_D (drag polar) for the trimmed aircraft. Those curves are very important to the aircraft performance determination.

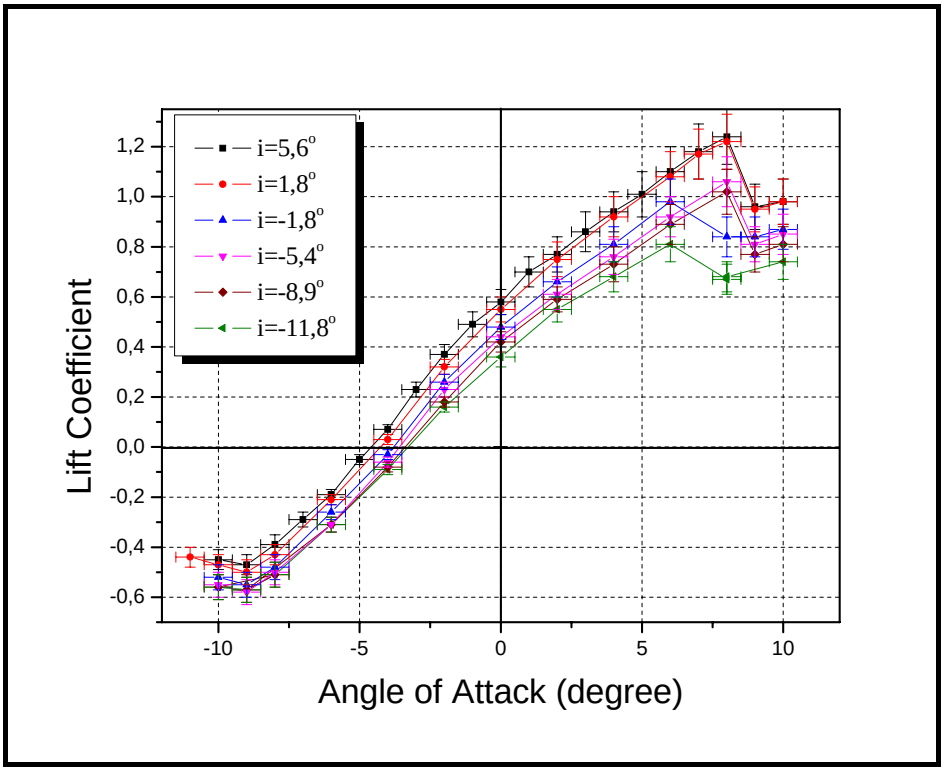

Figure 3: Lift coefficient as a function of the angle of attack, for the UAV complete configuration.

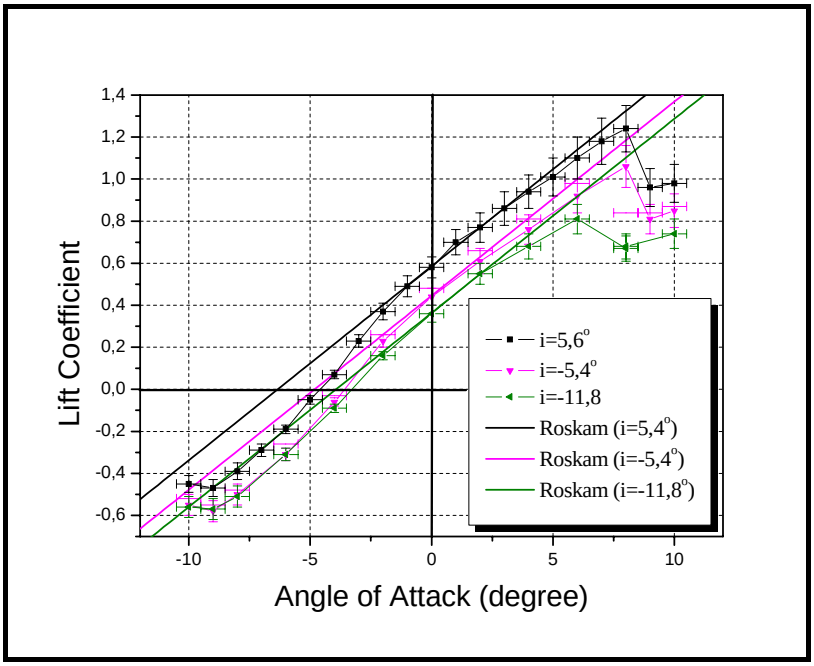

Figure 4: Lift coefficient as a function of the angle of attack: Comparison between experiments and theory.

Table 1: Comparison between experimental and theoretical values for the lift coefficient at zero angle of attack (C_{L_0}).

Horizontal tail Incidence angle	C_{L_0} **Theory**	C_{L_0} **Experiments**
5,6	0,6130	0,5607
1,8	0,5647	0,5080
-1,8	0,5189	0,4545
-5,4	0,4730	0,3862
-8,9	0,4285	0,3627
-11,8	0,3916	0,3258

The lift coefficient for several i_h values are shown in the Fig. 3, where an inflection of the linear part of the C_L curve can be observed. Such inflection was not detected for the wing-fuselage configuration (see Girardi et alli, 2007) and this result allows to conclude that inflection observed in the Fig. 3 is due to some interference caused by the horizontal tail. For angles of attack (α) greater than 0 degrees, the wake generated at the wing trailing edge flows over the horizontal tail surface. For $\alpha < 0$ degrees, such wake passes below the horizontal tail and this is a possible explanation for the behavior observed in the linear part of the lift curve.

The semi-empirical method presented by Roskam (2000) was applied to the complete configuration considered in the present paper and the results are shown in the Fig. 4, together with the experimental results. A good agreement can be observed for the linear part of the lift coefficient curve (where the semi-empirical method is valid), just for $\alpha > 0$ degrees and, in this situation, the wing wake is flowing in the region over the horizontal tail. A relative good agreement still can be observed for the lift coefficient for angle of attack equal to zero. The differences observed in the table 1 are a consequence of downwash angle theoretical estimation, performed by the semi-empirical method presented by Roskam (2000).

As will be presented bellow, the aircraft aerodynamic center is located at 174,5 mm from the aircraft nose (see table 2) and the model axis is located at 194,0 mm, that is, after the aerodynamic center. The average inclination of the near linear C_M x α curve (see Fig. 5) is a consequence of the model axis position, relative to the aerodynamic center. A behavior similar to the C_L x α curve can be observed in the pitch moment coefficient curve, shown in the Fig. 5 and a similar explanation can be considered, that is, the wing wake position relative to the horizontal tail. Such initial explanation will be confirmed in future works.

In order to perform the aircraft trim, the pitch moment coefficient must be calculated in relation to the aircraft gravity center (located at 158,0 mm from the aircraft nose) and this is easily performed by using a moment transformation equation, applied to the lift and pitch moment (relative to the model axis) coefficients for the same set of

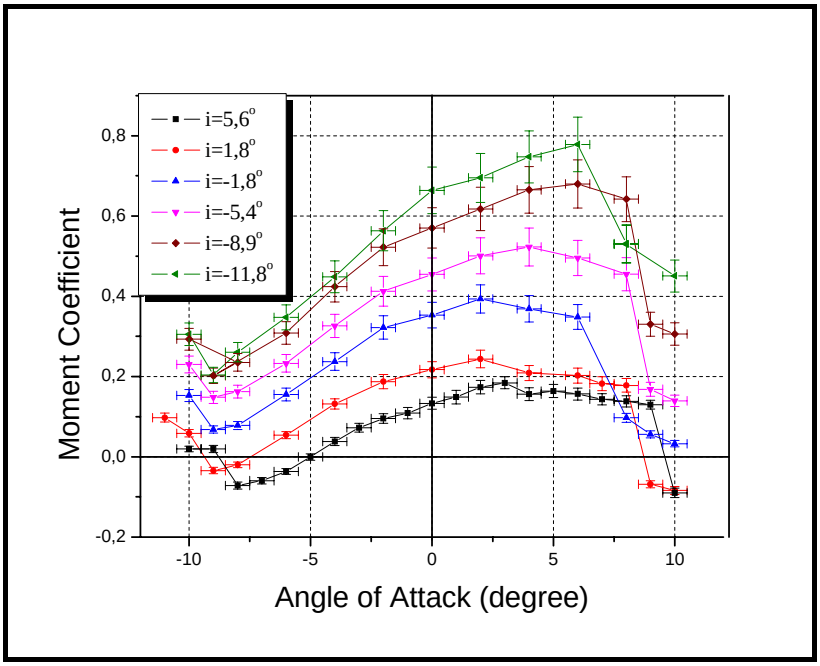

Figure 5: Pitch moment coefficient, related to the model axis, as a function of the angle of attack.

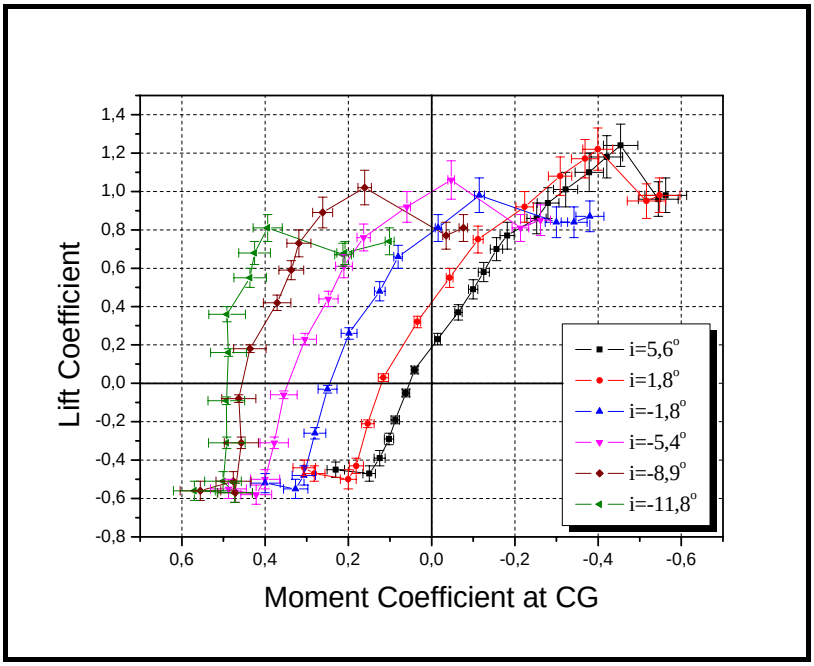

Figure 6: Lift coefficient as a function of Pitch moment coefficient, related to aircraft gravity center.

Table 2: Aerodynamic center position for the complete configuration.

Incidence	Aerodynamic center $\left(\overline{X}_{AC}\right)$
5,6	$0{,}52 \pm 0{,}04$
1,8	$0{,}52 \pm 0{,}05$
-1,8	$0{,}51 \pm 0{,}05$
-5,4	$0{,}46 \pm 0{,}04$
-8,9	$0{,}37 \pm 0{,}04$
-11,8	$0{,}34 \pm 0{,}04$

angle of attack. Once the static margin (difference between aerodynamic and gravity centers) is 18.5%, relative to the mean aerodynamic chord, the derivative $dC_{Mcg}/d\,C_L$ is negative (see Fig. 6) and the aircraft has a stable behavior.

Considering the lift and pitch moment coefficients as a function of the angle of attack, for each value of the horizontal tail incidence angle, the aerodynamic center of the aircraft complete configuration can be determined and for the present case, their value is shown in the table 2, where the X axis origin is at the wing aerodynamic chord leading edges and the mean aerodynamic chord is used to generate the non-dimensional position presented in the table 2. In the horizontal tail incidence angle, ranging from -5.4 to 5.6 degrees, the aerodynamic center position do not vary with i_h., as expected. For greater values of i_h, flow separation was observed at the horizontal tail and this is the cause for the aerodynamic center variation.

Considering the propulsive force do not impose pitch moment around the gravity center (the traction force is aligned with the aircraft gravity center), the aircraft is said trimmed when the pitch moment is zero and the aircraft lift coefficient can be determined in the Fig. 6, for each value of the horizontal tail incidence angle (i_h). Using the C_L values set, obtained above, and considering the corresponding C_L x α curve (for each value of i_h) the angle of attack the aircraft is trimmed is obtained for each value of i_h and then, the aircraft trimmed lift curve can be calculated, as presented in the Fig. 7.

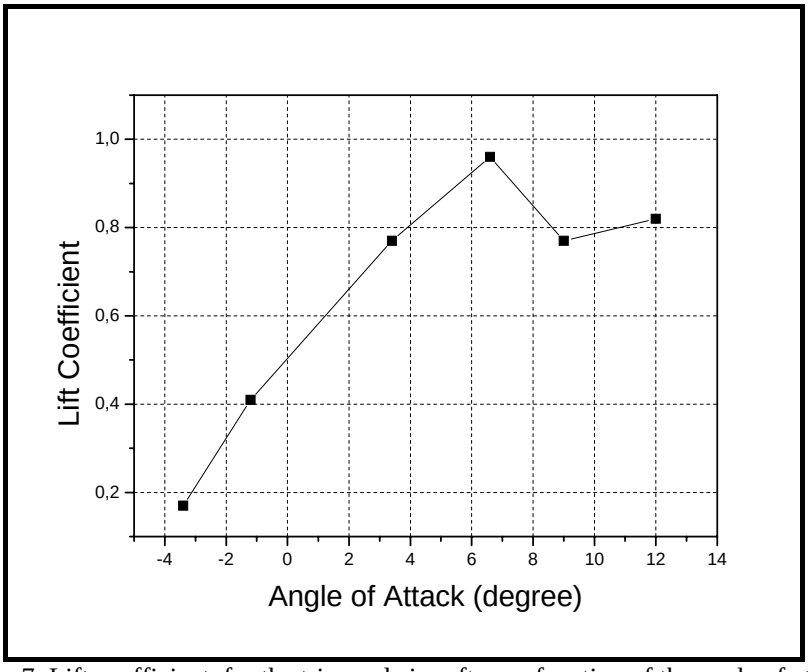

Figure 7: Lift coefficient, for the trimmed aircraft, as a function of the angle of attack.

The drag polar curve (C_L x C_D) is used extensively to obtain the aircraft performance, that is, the lift off and the landing runway lengths, the climb angle, the maximum cruise velocity, the service and absolute ceiling and curve performance are dependent on the drag polar. Such aerodynamic characteristic curve is a function of the aircraft geometric aspects, as well as, the surface roughness and the Reynolds number. Therefore, a different curve for each value of the horizontal tail incidence angle (i_h) has to be determined experimentally and the results, for the aircraft studied in this paper, are presented in the Fig. 8. For negative angles of attack it is possible to observe that the lowest values of C_D are obtained for horizontal tail incidence equal to 1.8 degrees. In this case, the lift generated at the horizontal tail is small and the induced drag of such lifting surface is very low, compared with the other configurations. For i_h values in the range between -5.4 and 5.6 degrees, the C_D growth, for a constant angle of attack, is low, showing the horizontal tail is working in the linear range of the lift curve, that is, no flow separation is observed at the tail surface. On the other hand, for i_h values equal to -8.9 and -11.8 degrees some flow separation is detected in the flow over the horizontal tail and an expressive C_D growth is observed (considering a constant angle of attack), for negative values of α. It is important to remember that for negative angles of attack (lower than – 5 degrees), the lift generated by the wing is negative and the flow at the horizontal tail region is influenced by the upwash velocity, induced by the wing wake, and the horizontal tail is subjected to a more negative effective angle of attack, associated to the separation behavior observed even for lower values of negative angle of attacks. On the other hand, for positive angle of attacks, downwash velocity is observed at the horizontal tail and, as a consequence, lower effective angle of attacks, which are correlated to a non-separated behavior observed for $\alpha > 0$ degrees.

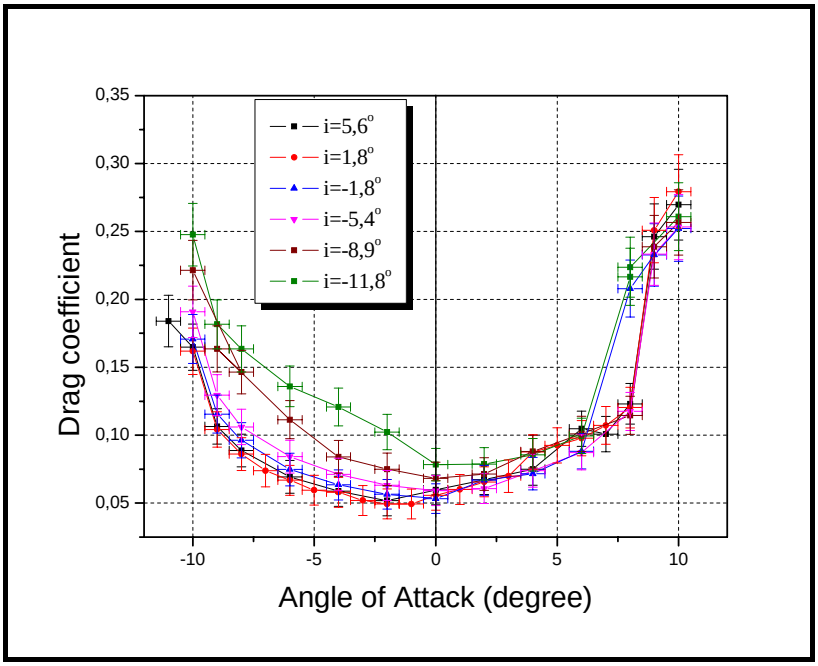

Figure 8: Drag coefficient as a function of the angle of attack.

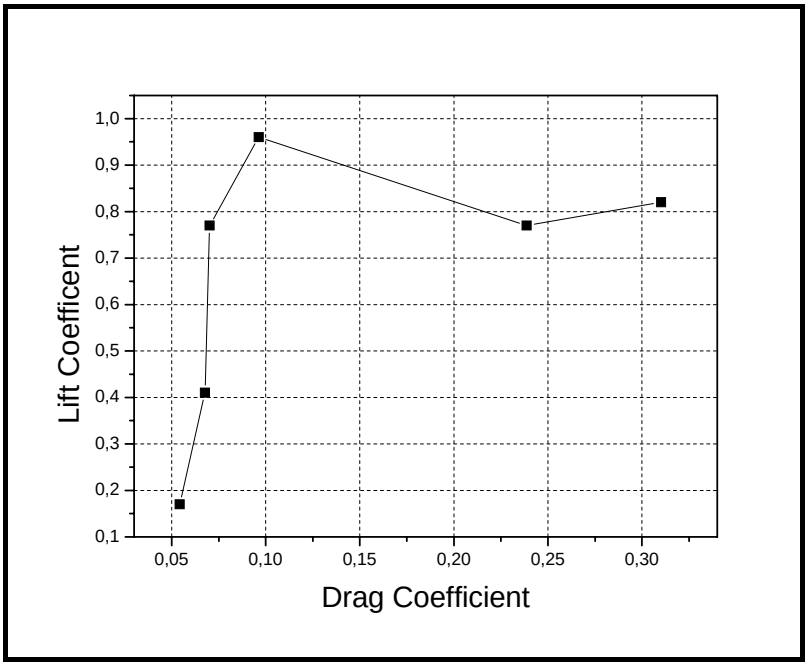

Figure 9: Drag polar for the trimmed aircraft.

The above polar drag curves were obtained for a model with fixed configuration and therefore, just one point of each curve is used to describe the trimmed aircraft. As described above, for each value of i_h a value of C_L is obtained when the pitch moment (related to the gravity center) coefficient is equal to zero. In a second step, considering the corresponding C_L x α curves, an angle of attack is associated to each value of C_L. In the third step, the corresponding (for the same value of i_h) C_D x α curves, shown in the Fig. 8, a value of C_D is associated to the value of C_L and a trimmed drag polar (see Fig. 9) is determined to the aircraft studied in this work.

5. FINAL REMARKS

The complete configuration of the UAV developed at ITA was analyzed experimentally in the present work with the following objectives: (i) Determination of the lift coefficient (C_L x α) and the drag polar (C_L x C_D) curves for the trimmed aircraft, in order to perform the aircraft performance, (ii) the aerodynamic center position, required to the

aircraft stability analysis and to determine the elevator angle and the aircraft angle of attack in the trimmed condition and (iii) the evaluation of part of the semi-empirical method normally implemented in the aircraft conceptual design phase.

A great amount of experimental data was obtained in this research program and just the preliminary analysis of such data was performed in the present paper. All the aerodynamic characteristic curves were obtained experimentally and in some cases the semi-empirical method was applied to the studied configuration and compared with the experiments. The differences between experiments and semi-empirical method were a consequence of errors in the formula used to calculate the downwash variation with the aircraft angle of attack. In future works, a simple numerical code (vortex lattice method) will be implemented to improve determination of the downwash angle (generated by the wing) at the horizontal tail and its variation with the aircraft angle of attack.

Some points of the C_L x α and the drag polar (C_L x C_D) for the trimmed aircraft were determined and preliminary calculations can be performed to obtain the aircraft performance. Some uncertainties were detected on the experimental results and they were caused by the sensors used to determine the lift and pitch moment. In future works, more flexible load cells will be used and more accurate experimental results will be obtained. More horizontal tail incidence angles will be tested in order to obtain more resolution for the aerodynamic characteristic curves.

6. ACKNOWLEDGEMENTS

To the Financiadora de Estudos e Projetos (FINEP), for supporting part of the resources used to the Unmanned Aircraft Vehicle development (protocolo 243/2004) and to the Centro de Estudos de Sistemas Avançados do Recife (CESAR), to the partnership in this project. To the staff of the Prof. K.L. Feng Aeronautical Engineering Laboratory: Carlos Guedes Neto, Luis Zambrano Lara, Vitor Valentim Betti and Mario Correia.

7. REFERENCES

Bearman, P.W. (1965): Investigation of the flow behind a two-dimensional model with a blunt trailing edge and fitted with splitter plates. *J. Fluid Mech*., Vol. 28, pp. 241-255.

Girardi, R.M. e Rizzi, P., (2005a), "Análise do tipo da aeronave mais adaptada para a inspeção de linhas de transmissão", Relatório de Trabalho, CESAR/ITA, 27 de junho.

Girardi, R.M. e Rizzi, P., (2005b), "Seleção da alternativa mais promissora para prova de conceito, através da construção e testes em vôo", Relatório de Trabalho, CESAR/ITA, 27 de junho.

Girardi, R.M. e Rizzi, P., (2006), "Desenvolvimento de Metodologia para Projeto Conceitual de um Veículo Aéreo Não Tripulado (VANT), Usado para Inspeção de Linhas de Transmissão de Energia Elétrica", Anais do Congresso Nacional de Engenharia Mecânica (CONEM), Recife, Pe.

Girardi, R.M. e Rizzi, P., (2006), "Projeto Conceitual de um Veículo Aéreo Não tripulado, Usado para Inspeção de Linhas de Transmissão de Energia Elétrica". Anais do 11º Encontro Nacional de Ciências e Engenharia Térmicas (ENCIT 2006), Curitiba, Dez. 5-8.

Kline, S.J. and McClintock, F. A. (1953): Describing uncertainties in single-sample experiments. *Mechanical Eng*., pp. 3-8.

Kubo,Y. et all.(1989): Effects of end plates and blockage of structural members on drag forces. *J. Wind Eng. Ind. Aerodynamics*, vol.32, pp.329-342.

Rae, W.H. and Pope (1984), A *Low speed wind tunnel testing*. Second edition, John Wiley & Sons, USA.

Raymer, D.P., (1999), "Aircraft design: a conceptual approach", AIAA Education Series, AIAA, Washington DC.

Roskam, J., (2000-2003), "Airplane design", parts I-VIII, Dar Corporation, Lawrence, Kansas, USA.

8. RESPONSIBILITY NOTICE

The authors are the only responsible for the printed material included in this paper.